

Ultrasonic Characterization of Extra-Cellular Matrix in Decellularized Murine Kidney and Liver

L. A. Wirtzfeld, E. S. L. Berndl, M. C. Kolios
 Department of Physics
 Ryerson University
 Toronto, Canada
 mkolios@ryerson.ca

Abstract— Three-dimensional scaffolds are essential to the field of tissue engineering. While novel synthetic structures are being developed, there is still a great interest in exploring natural scaffolds in tissue, the extra-cellular matrix (ECM). A recently developed technique known as “decellularizing” allows for the removal of cells from intact tissue while preserving the ECM structure. In order to exploit the uniqueness of the native ECM, a structure which varies significantly between organs, it first needs to be well studied. This study outlines the use of quantitative ultrasound as a non-destructive method to characterize the extracellular matrix of excised murine kidneys and livers. This allows for the study of both natural tissue scaffolds, as well as the contributions of the cellular and extra-cellular components to ultrasound backscatter. In this study, excised murine livers and kidneys were imaged with a VisualSonics Vevo2100 using nominal 40 MHz linear-array transducer, after being maintained in PBS. Subsequently the organs were decellularized, in this process, the ECM of the tissue is isolated from its inhabiting cells, leaving an ECM scaffold of the tissue. The remaining extra-cellular matrix structures were reimaged. Raw RF data was acquired and normalized by a reference phantom. Linear fits to the normalized power spectra allow for the estimation and comparison of the spectral slope and midband fit. After being decellularized, the organs were significantly smaller in volume with increased backscatter in the liver and overall decrease in the kidney. The heterogeneous structure of the kidney was apparent in parametric images, with the spectral slope and midband fit higher in the central medulla region. The ability to compare backscatter from the extracellular matrix with and without cells allows for a detailed analysis of the contribution of individual cells to the ultrasound backscatter and could be employed to evaluate scaffold structures and progress of growth on these scaffolds.

Keywords—*Extracellular matrix, high-frequency ultrasound, quantitative ultrasound*

I. INTRODUCTION

Three-dimensional biocompatible scaffolds for the growth of cells are essential to the field of tissue engineering. While novel synthetic structures are being developed, there is still a great interest in exploring the natural scaffolds in tissue, the extra-cellular matrix (ECM), both to better understand the function and cellular interactions, and also as a potential scaffold for tissue regeneration that could avoid immune reaction [1,2]. A recently developed technique [3] known as “decellularizing” allows for the removal of cells from intact tissue while preserving the ECM structure. In order to exploit

the unique nature of the native ECM, a structure which varies significantly between organs, it first needs to be well characterized.

The fundamental sources of ultrasound scattering in tissue has been extensively studied, with particular emphasis on the contributions from the cell and the cell nucleus. The extracellular matrix likely to contribute to ultrasound backscatter, but it is challenging to isolate its contributions to tissue scatter from the cellular scattering.

This study outlines the use of quantitative ultrasound as a non-destructive method to characterize the extracellular matrix of excised murine kidneys and livers. This allows for the study of both natural tissue scaffolds, as well as the contributions of the cellular and extra-cellular components to ultrasound backscatter.

II. METHODS

Four Kidneys and two livers were excised, post-mortem, from two male SCID-CB-17 (Charles River). Organs were placed in PBS for approximately 30 minutes to remove large debris and preserve the organs during transportation.

A. Decellularization

The organs were decellularized using the technique developed by Ott et al. [3] to remove the cells while preserving the extracellular matrix within the organ. After imaging, organs were placed in bath of 1% Sodium dodecyl sulfate (SDS) at

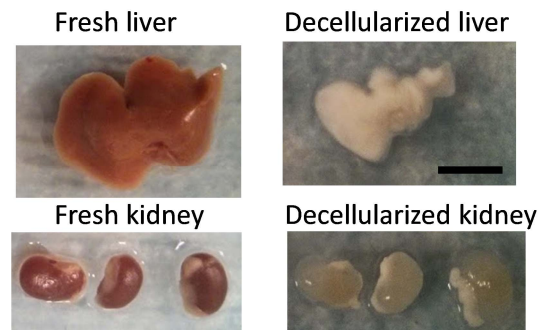


Fig. 1. Examples of fresh (left) and decellularized (right) liver (top) and kidneys (bottom). Scale bar is approximately 1 cm, not exact due to camera angle.

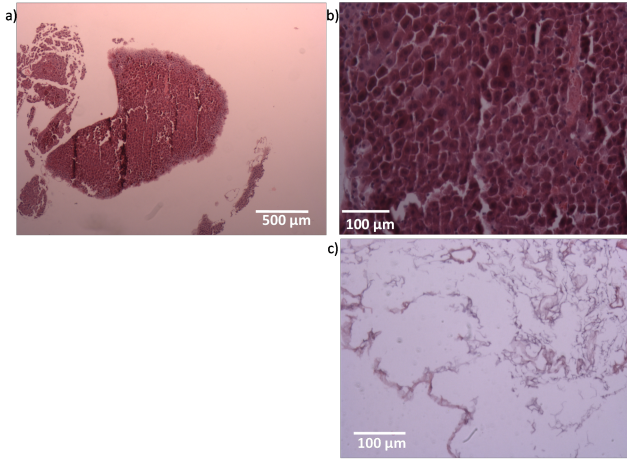


Fig. 2. H&E stained histology slides of a liver: fresh (a,b) and decellularized (c). Change in gross structure can be seen due to decellularization at both low magnification (a,c) and at high magnification (b,d) where the basic shape of the tubules and glomeruli still remain.

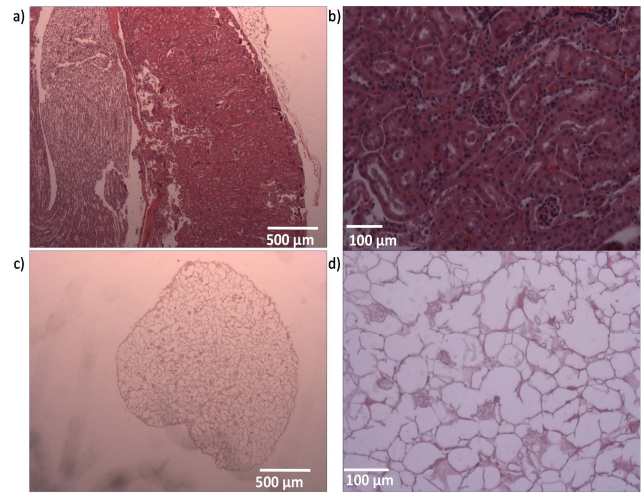


Fig. 3. H&E stained histology slides of a kidney: fresh (a,b) and decellularized (c, d). Change in gross structure can be seen due to decellularization at both low magnification (a,c) and at high magnification (b,d) where the basic shape of the tubules and glomeruli still remain.

room temperature, with gentle stirring, and covered with Parafilm for approximately 72 hours. SDS was changed approximately every 12 to 24 hours, when the solution became cloudy. SDS was then replaced with 1% Triton X with stirring for approximately 3 hours, followed by PBS for 1 to 2 hours, until the organs were imaged a second time.

B. Histology

Additional sample organs, either fresh or decellularized, were placed in 10% neutral buffered formalin (NBF) for two to five days, then placed into paraffin blocks, and cut into 6 μm sections. Slides were stained with hematoxylin and eosin (H&E). Matched organs were used for the fresh and decellularized histological samples, with the first half of the organ placed in NBF fresh and the second half placed after being decellularized.

C. Ultrasound Imaging

Organs were imaged at two time points, first after excision when the tissue was intact and fresh and a second time after being decellularized. Organs were affixed to a small piece of PlexiGlas using a cyanoacrylate adhesive to immobilize them for ultrasound imaging and placed in a PBS bath at room temperature. The organs were imaged with a Vevo2100

(Fujifilm VisualSonics Inc., ON, Canada) and a MS550S linear array transducer. A single 6 mm transmit focus was used. Data were acquired in 3D-RF mode, with a step size of 76 μm over a 10.1 mm range, to acquire data from across the entire organ.

After imaging the organs, matched data was acquired from a well characterized reference phantom using the same imaging settings as were employed for the organs.

D. Data Analysis

Analysis was performed on the odd numbered slices from the 3D data set that were within the body of the organ. Offline, the organs were manually segmented. For the kidneys, the regions for the adrenal, cortex and medulla were also manually outlined to allow a comparison between these regions. The outlined regions were automatically sub-divided into overlapping analysis regions 880 μm x 880 μm (approximately 16 scan lines by 10 pulse lengths) to perform further analysis. Data was processed over a bandwidth of 15 MHz to 35 MHz. Within each analysis window, the power spectrum was computed for each scan line and the backscatter coefficient (BSC) calculated using the depth matched reference phantom data and the reference phantom method described in [4]. Two fitting methods were used to estimate parameters, first a linear

TABLE I. ULTRASOUND BASED PARAMETER ESTIMATES FOR THE LIVER, KIDNEY AND SUB-REGIONS OF THE KIDNEY. BOTH FRESH AND DECELLULARIZED TISSUE RESULTS ARE SUMMARIZED. VALUES ARE MEAN (ACROSS ALL 2D PLANES AND ALL ORGANS) \pm THE STANDARD DEVIATION

	Slope (dB/MHz)		Midband Fit (dB)		ESD (μm)	
	Fresh	Decellularized	Fresh	Decellularized.	Fresh	Decellularized
Liver	0.38 \pm 0.34	0.35 \pm 0.42	-25.1 \pm 5.5	-16.2 \pm 9.1	17.3 \pm 7.9	18.8 \pm 8.0
Kidney (average)	0.29 \pm 0.10	0.40 \pm 0.14	-29.8 \pm 2.8	-35.8 \pm 5.1	18.6 \pm 2.7	16.2 \pm 2.8
Kidney (cortex)	0.28 \pm 0.10	0.43 \pm 0.15	-29.9 \pm 2.8	-37.8 \pm 3.8	18.7 \pm 2.7	15.7 \pm 2.8
Kidney (medulla)	0.46 \pm 0.11	0.34 \pm 0.09	-31.0 \pm 4.0	-34.8 \pm 3.8	15.3 \pm 3.8	18.2 \pm 2.6
Kidney (adrenal)	0.14 \pm 0.09	0.17 \pm 0.26	-19.6 \pm 4.2	-19.6 \pm 6.4	23.1 \pm 1.3	21.0 \pm 4.4

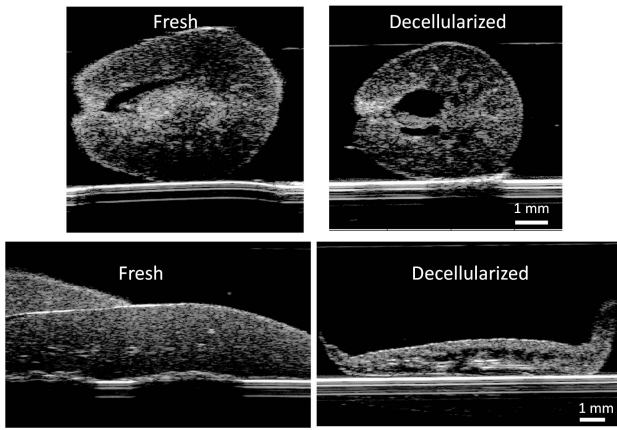


Fig. 4. High-frequency B-mode ultrasound images of a cross-section through the centre of a kidney (top) and across a liver (bottom). Both the organs were imaged fresh (left) and after being decellularized (right). Changes in speckle appearance and overall size can be observed. 2D images selected to be approximately same location within 3D image for comparison. Scale bars 1 mm.

fit was applied to the BSC to estimate the spectral slope and midband fit over the bandwidth [5]. Second, a fluid filled sphere model was fit to the BSC to provide an estimate of the effective scatterer diameter [6].

III. RESULTS AND DISCUSSION

After being decellularized the organs were smaller in volume with a loss of tissue color. The liver appeared white and the kidney more heterogeneous with white and translucent

regions, as seen in Fig. 1. The liver decreased in size substantially and the kidneys decreased in size slightly. The histological change in appearance of the liver and kidney are shown in Fig. 2 and Fig. 3, respectively. The liver has limited structure after being decellularized (Fig. 2). In comparison, the kidney, in Fig. 3, has visible structure after being decellularized including open regions that likely correspond to the location of tubules and smaller denser regions that likely correspond to the location of glomeruli.

For the liver and each of the regions of the kidney, the estimated effective scatterer diameter from the fluid filled sphere model, and the estimated midband fit and spectral slope for the liver and kidney are summarized in Table I. The MBF from the livers increased after being decellularized, while the kidneys decreased on average. Within the kidneys, the greatest decrease in MBF was seen in the cortex, followed by the medulla and the adrenal region remained consistent.

The standard deviations were relatively high for some estimates across all 2D slices and all organs imaged. This may be a result of limitations in outlining the different regions manually based on B-mode image appearance. There is also the possibility of variations in the state of the ECM after being decellularized as the process was performed with mixing in a flask rather than via organ perfusion.

The spectral slope estimate for the liver had a higher standard deviation than change in the estimate. For the kidney, there was an increase in spectral slope after being decellularized in the cortex and in the adrenal region. For the medulla there was decrease. The differences in structure and

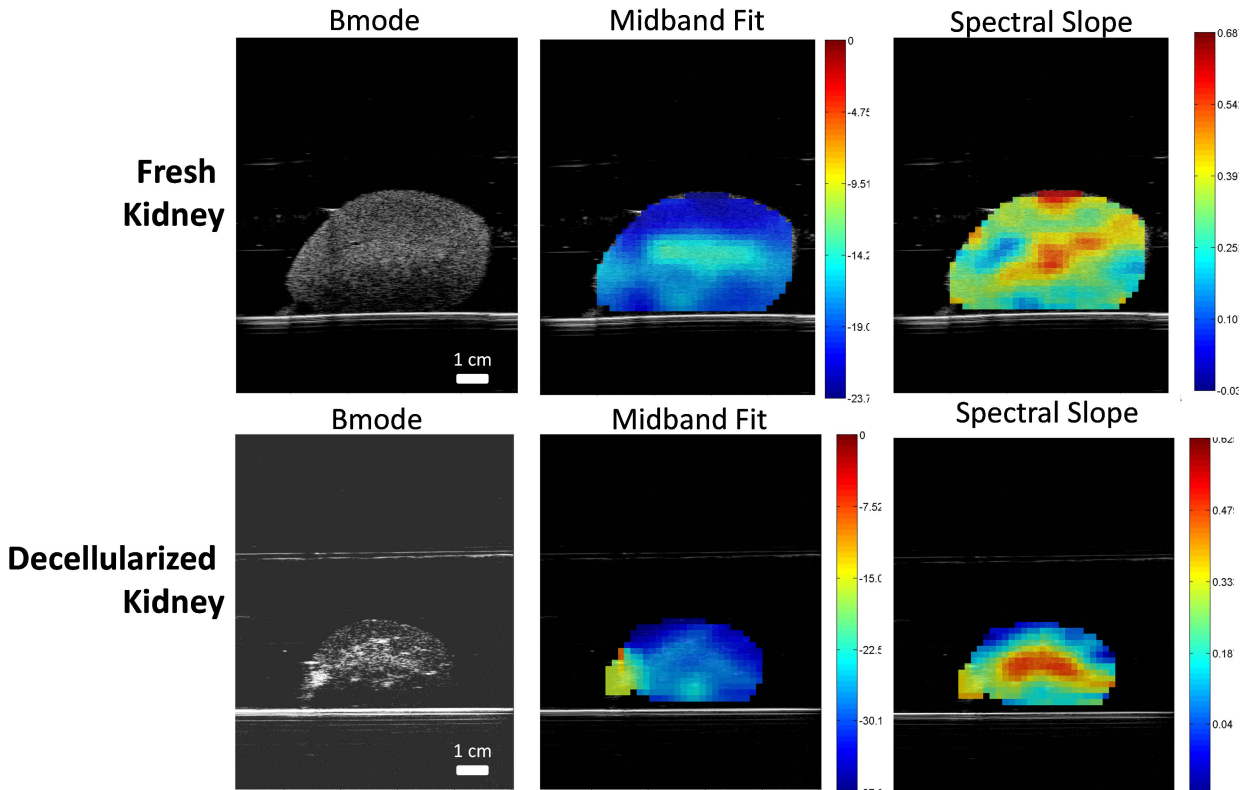


Fig. 5. Columns show the Bmode, parametric midband fit (dB) and spectral slope (dB/MHz) images of an excised murine kidney fresh after excision (top) and after being decellularized (bottom). Relative change in size and parameter heterogeneity can be observed. Colorbars scaled to observed parameter ranges.

how cellular these regions are may be the cause of these different trends.

There are variations in the average estimated ESD (Table I), but they are generally on the order of the standard deviation. Despite the lack of cells to contribute to the ultrasound scattering after being decellularized, it was consistently observed that there is still enough structure to scatter the ultrasound and allow for parameter estimation. In particular, the ESD needs to be further investigated to understand how the structure would relate to the obtained estimates.

An example of a heterogeneous 2D image of the kidney is shown in Figure 5. Parametric images are shown of the spectral slope and midband fit slightly higher in the central medulla region. This heterogeneity is also seen in the decellularized organs. The summarized estimates (Table I) across all slices and organs have higher variability and therefore distinct values for the medulla and cortex are not observed. This may be in part due to the challenges of segmenting out different regions based on the B-mode images and the fact that the heterogeneity is gradual rather than the values changing abruptly at an interface.

IV. CONCLUSIONS

Variations in ultrasound parameters across the different regions of the kidney continued to be observed after being decellularized where the only structure left to contribute to the ultrasound scattering and structure of the organ is the ECM. These variations across regions of the kidney and between the kidney and liver suggest that the ECM is contributing to ultrasound scattering in addition to the cellular structures often explored.

The ability to non-invasively monitor subtle changes in the ECM structure and differentiate between cellular and decellular organs, offers the potential for ultrasound imaging to be used in the assessment of tissue engineered constructs and to monitor tissue regeneration within the scaffolds.

ACKNOWLEDGEMENTS

The authors would like to acknowledge funding to support this work from Canada Foundation for Innovation, the Canada Research Chairs and The Terry Fox New Frontiers Program Project Grant in Ultrasound and MRI for Cancer Therapy (project #1034).

REFERENCES

- [1] S. F. Badylak, "The extracellular matrix as a biologic scaffold material.," *Biomaterials*, vol. 28, no. 25, pp. 3587–93, Sep. 2007.
- [2] P. M. Crapo, T. W. Gilbert, and S. F. Badylak, "An overview of tissue and whole organ decellularization processes.," *Biomaterials*, vol. 32, no. 12, pp. 3233–43, Apr. 2011
- [3] H. C. Ott, T. S. Matthiesen, S.-K. Goh, L. D. Black, S. M. Kren, T. I. Netoff, and D. A. Taylor, "Perfusion-decellularized matrix: using nature's platform to engineer a bioartificial heart," *Nat Med*, vol. 14, no. 2, pp. 213–221, Feb. 2008.
- [4] L. X. Yao, J. A. Zagzebski, and E. L. Madsen, "Backscatter coefficient measurements using a reference phantom to extract depth dependent instrumentation factors," *Ultrason. Imaging*, vol. 12, no. 1, pp. 58–70, 1990.
- [5] F. L. Lizzi, M. Greenebaum, E. J. Feleppa, M. Elbaum, and D. J. Coleman, "Theoretical framework for spectrum analysis in ultrasonic tissue characterization," *J. Acoust. Soc. Am.*, vol. 73, no. 4, pp. 1366–1373, Apr. 1983.
- [6] M. F. Insana, R. F. Wagner, D. G. Brown, and T. J. Hall, "Describing small-scale structure in random media using pulse-echo ultrasound," *J Acoust Soc Am*, vol. 87, no. 1, pp. 179–192, Jan. 1990.